An Easy Procedure for Calibrating Data Acquisition Systems Using Interleaving

Filomena M. C. Clemêncio, Custódio F. M. Loureiro, and Carlos M. B. A. Correia

***Abstract*—Interleaving data acquisition channels is a well-known and interesting technique to achieve higher acquisition rates. However, to obtain the expected benefits, a careful look at the interleaving technique and to mismatches that can lead to unwanted harmonic distortion and noise is essential.**

In this paper we discuss the methods used to interleave existing high-speed, 250 MSPS 8-bit acquisition channels, and the results obtained. The methods presented allowed a good relative channel calibration in amplitude (amplitude mismatch under 0.1 lsb) and in time (time mismatch between acquisition channels in the ps range, under the specified maximum jitter for the ADC used).

A dynamic, by software, amplitude level signal-dependent adjustment procedure is also suggested for signals with rich frequency content that can substantially improve the quality of the acquired signal when using interleaved channels.

The techniques presented provide good results even in the presence of noise.

***Index Terms*—Data acquisition, interleaved systems.**

I. Introduction

In this work we discuss the methods used to interleave existing high-speed acquisition channels [1] in use in the reflectometry diagnostic in tokamak ASDEX-Upgrade [2] and the results obtained.

Each data acquisition module in the diagnostic consists of four independent 250 MSPS 8-bit acquisition channels (ACs) that can be interleaved to reach higher sampling frequencies and deeper memory. A simplified block diagram of the module can be seen in Fig. 1 and its physical organization in Fig. 2. In Fig. 3, a photograph of the actual hardware is shown (component side; the module has two ACs built in the solder side).

Each analog input to the module has a 50 ohm impedance controlled line. The interleaving of the different ACs is achieved by routing the analog signal through the desired ACs and by terminating the line with the appropriate impedance.

II. Basic Theory

Interleaving data acquisition channels usually incurs in mismatch-related problems that lead to unwanted harmonic distortion and noise. The basic sources of error are temporal mismatches, which lead to nonuniform sampling, and amplitude mismatches, which lead to noisy acquired signals. To complicate things a little bit there are usually frequency dependent mismatches in the analog front end (seen here as formed by the analog amplification/formatting stage followed by the data conversion stage) of the interleaved channels, and a method to correct dynamically these errors would be a benefit.

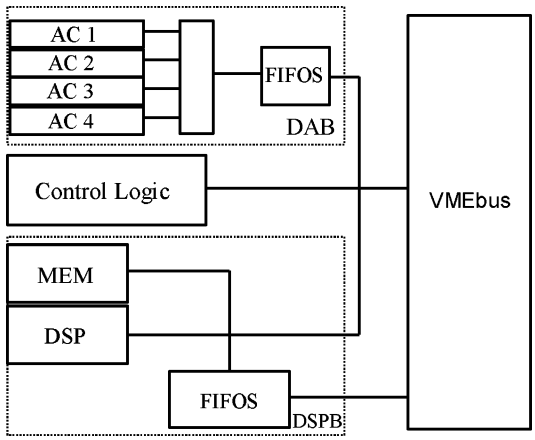

Fig. 1. Simplified block diagram of the data acquisition module.

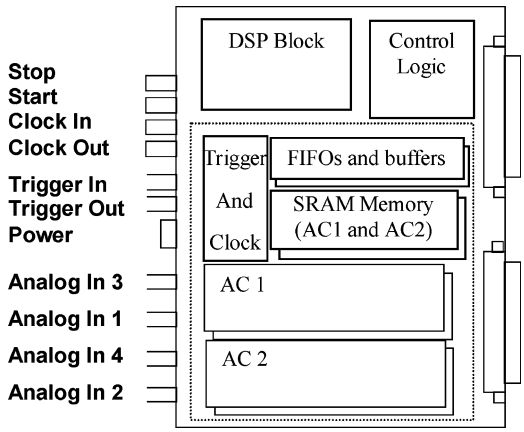

Fig. 2. Physical organization of the data acquisition module.

A. Strategy

When interleaving data acquisition channels a first question must be answered: should we treat the acquired data as one channel and try to identify and correct the different mismatches, or should we use a priori the knowledge that data is being acquired by several interleaved channels?

In this work we took the last approach. The reasoning is the following: each AC should see exactly the same signal (except for a small phase delay), as each channel acquires independently the same analog signal but delayed by T/n, with n the number

Manuscript received October 6, 2006; revised May 25, 2007.

F. M. C. Clemêncio is with the Escola Superior de Tecnologia da Saúde do Porto, 4000-294 Porto, Portugal (e-mail: fcc@estsp.ipp.pt).

C. F. M. Loureiro and C. M. B. A. Correia are with the Department of Physics, CEI, University of Coimbra, P-3004-516 Coimbra, Portugal (e-mail: custodio@fis.uc.pt; correia@fis.uc.pt).

Digital Object Identifier 10.1109/TNS.2007.903166

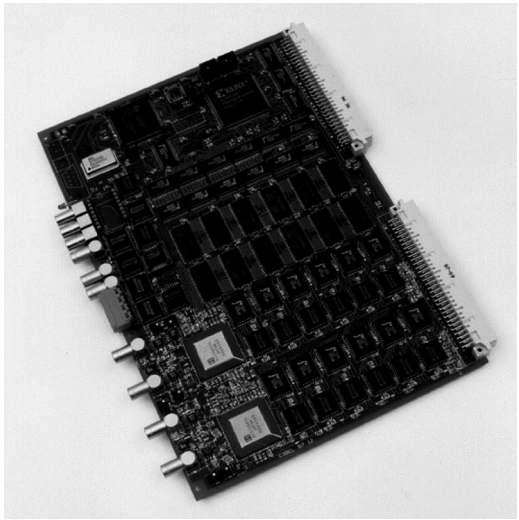

Fig. 3. Photograph of the developed module (component side).

of interleaved ACs, and T the master sampling clock. It is expected that delaying the input signal by at most one period of the sampling clock (or a smaller fraction of a period) will not substantially change its characteristics, and so the problem reduces to one of accurately measuring the characteristics of an acquired signal. For that we shall rely on the discrete Fourier Transform (DFT) and on interpolating the DFT coefficients.

B. Interpolating the DFT Coefficients

A fast and well-known method for measuring the parameters that characterize a given signal is based on the evaluation of its spectral components, achieved effectively through the FFT algorithm. In practice, however, some care must be taken to avoid the well-known problems of spectral leakage, due to a finite measurement length, and of the granularity of the obtained DFT spectrum, due to sampling. The standard answers to these problems are the use of windows [3], [4] and the interpolating of the DFT coefficients.

A set of interpolating formulae to use with an Hann window is found in [5]. These formulae were used in this work. They are as follows.

Consider a sampled multifrequency signal:

$$x(kT) = \sum_{m=1}^{M} A_m \sin(2\pi\nu_m kT + \varphi_m) \quad k = 0, 1, \ldots, N-1$$

where M is the number of frequencies composing the signal, and $\mathrm{A_m}$, ν_m, φ_m the amplitude, frequency and phase of the m frequency component of the signal, and T the sampling period.

After calculating the spectra X(n) of the sampled signal through the FFT algorithm, a peak search procedure is used to find the index m of each independent spectral line. The true frequency ν_m of the corresponding component frequency is given by:

$$\nu_m = (m+\delta_m)\frac{1}{NT} \quad \delta_m = \frac{2\alpha_m - 1}{\alpha_m + 1} \quad \alpha_m = \frac{|X(m+1)|}{|X(m)|}.$$

where δ_m is the fractional bin deviation and α_m is derived based on the magnitude of the m and $\mathrm{m}+1$ spectral lines.

The following formulae are used for the amplitude and phase of the different spectral components and also for the true dc value of the signal. Note that [5] deduces, in some cases, two different expressions, suggesting the use of the one for which the spectral line has the larger amplitude.

Amplitude interpolating formulae:

$$A_m = \frac{2\pi\delta_m(1-\delta_m)}{\sin(\pi\delta_m)} e^{-j\pi\delta_m}(1+\delta_m)X(m)$$
$$A_m = \frac{2\pi\delta_m(1-\delta_m)}{\sin(\pi\delta_m)} e^{-j\pi\delta_m}(\delta_m-2)X(m+1).$$

Phase interpolating formulae:

$$\varphi_m = Phase\{X(m)\} - \pi\frac{N-1}{N}\delta_m + \frac{\pi}{2}$$
$$\varphi_m = Phase\{X(m+1)\} - \pi\frac{N-1}{N}(\delta_m - 1) + \frac{\pi}{2}.$$

True dc value of the signal interpolating formula:

$$V_{dc} = \frac{X(0)}{N} - \frac{1}{N}\sum_{m=1}^{M} A_m \frac{\sin(\pi\lambda_m)}{\sin\left(\frac{\pi\lambda_m}{N}\right)} \sin\left(\pi\frac{N-1}{N}\lambda_m + \varphi_m\right).$$

C. Applicability of the Method

Due to the good behavior of the interpolation method in what concerns systematic errors and noise sensibility [5], [6] and the fact that the method does not rely on a priori temporal information (temporal information is added during the interpolation process after the FFT algorithm) the proposed calibrating procedure can be used with modern higher-speed higher-resolution data acquisition systems using interleaving.

III. Experimental Setup

Testing software was developed in C++ under Windows that allow a quick inspection of the fundamental characteristics of the data acquisition channels, and fast adjustment of the offset and gain of each channel. Appropriately terminated transmission lines are driven from a passive splitter and used to distribute the analog input signal to the different acquisition channels, and are also used to control the data acquisition time in each channel. The test software allows measuring the time lag between the different acquisition channels with picosecond resolution, and the length of the analog transmission lines is adapted accordingly to

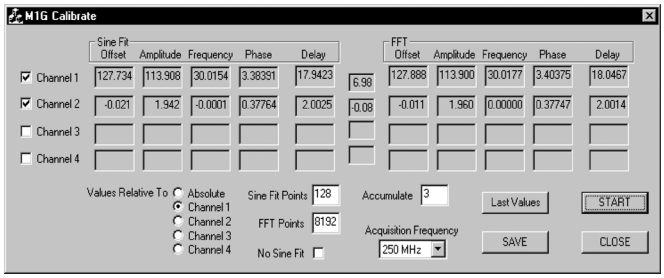

Fig. 4. The test calibration software.

optimize the response of the overall channel to a given calibration frequency. After these adjustments the interleaved channels can be measured.

A set of test sinusoids, with frequencies up to 250 MHz, were generated using a ROHDE&SCHWARZ SWEEP GENERATOR 0.4...2500 MHZ SWP. Each test frequency was conveniently filtered using an appropriate filter (Mini-Circuits Model BLP-1.9).

The calibrating software (Fig. 4) uses a peak search algorithm and the algorithms in [5] to do DFT interpolation. It also implements a least square fit to the sinusoidal signal, allowing a quick result comparison of both methods. The number of waveform points used in the sine fit and in the DFT can differ (useful as the sine fit algorithm is very computationally intensive). An option is also provided for showing the mean of several measurements. Results are exclusively based on the quantized data acquired on each channel and on the acquisition frequency chosen. The Delay shown is based on the calculated phase and has units of nanosecond. In between the set of numbers calculated through the sine fit and DFT algorithms is the measured effective number of bits (ENOB).

For test frequencies over the Nyquist range the aliased (folded-back) frequency is used. Again this frequency should be seen with the same fundamental characteristics in all interleaved channels.

IV. Experimental Results

The acquisition channels were initially characterized independently. Two interleaved acquisition channels were then characterized and compared to an individual channel and several remarks drawn. Finally several multifrequency signals were acquired and shown in the time domain.

All signals were acquired with each channel operating at the maximum allowed sampling frequency of 250 MHz. The ADC in use is the Harris HI1166.

In order to allow for the representation on the same graph of the Equivalent Number of Bits (ENOB), the Total Harmonic Distribution (THD), and the Spurious Free Dynamic Range (SFDR), the well-known formula

$$ENOB = \frac{(SNR - 1.76)}{6.02}$$

is used to convert from the usual units of dB of the corresponding signal-to-noise ratio (SNR) to the units of bit used in the plots.

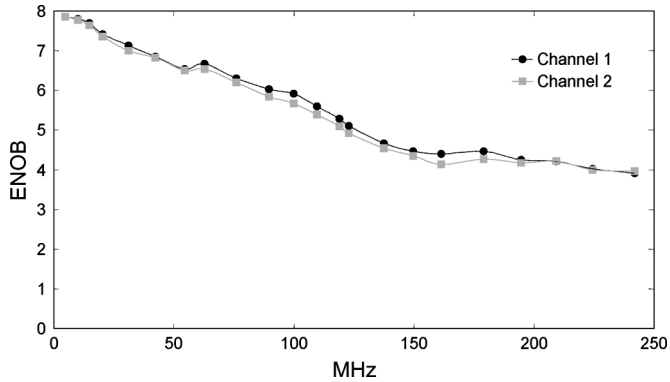

Fig. 5. ENOB versus input sinusoid frequency (full scale input).

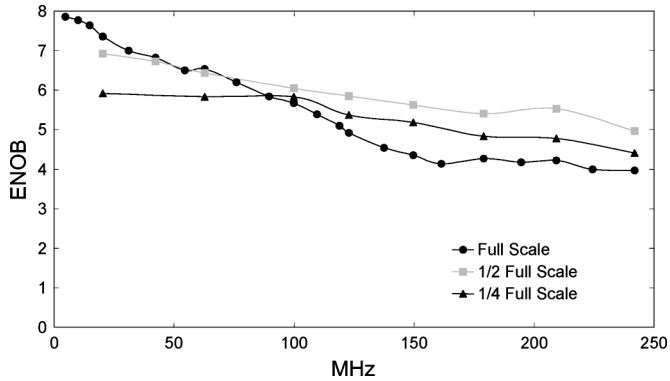

Fig. 6. ENOB versus input sinusoid frequency (signals with different amplitudes).

A. Independent Channels

Data are shown characterizing acquisition channels 1 and 2 (the other acquisition channels have a similar behavior). Full scale and 1/2 and 1/4 full scale sinusoidal signals were used.

Fig. 5 shows the full scale ENOB versus input sinusoid frequency, whereas in Fig. 6 the ENOB behavior with input sinusoids of lesser amplitude is shown.

In general, the data acquisition channels show a very good performance at low input frequencies, with an ENOB bigger than 7.6 bits (full scale input) up to 15 MHz sinusoids. Up to approximately 80 MHz the ENOB is over 6 bits. At the Nyquist frequency the ENOB is close to 5 bits, reducing slowly to 4 bits at 225 MHz. The ENOB reduction is much gentler for signals with lower amplitude, suggesting a good performance when acquiring signals with fast but relatively small amplitude transitions.

In Fig. 7, an idea is given of the relative importance of harmonic and spurious contributions to the ENOB.

No cross-talk effects could be measured between channels.

B. Interleaved Channels

The two channels were interleaved and calibrated with the test software referred in Section III. We found experimentally that, for a given sinusoid frequency, the amplitude accuracy achieved when comparing channels is under 0.1 lsb, and the uncertainty in the time lag between channels is in the picosecond range, well under the 9 ps jitter specified by the manufacturer of the ADC.

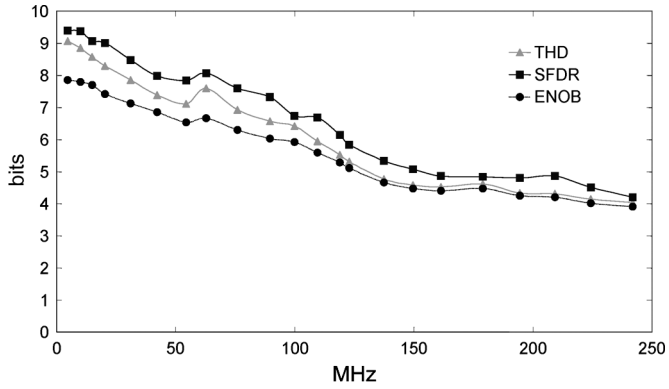

Fig. 7. ENOB, THD and SFDR.

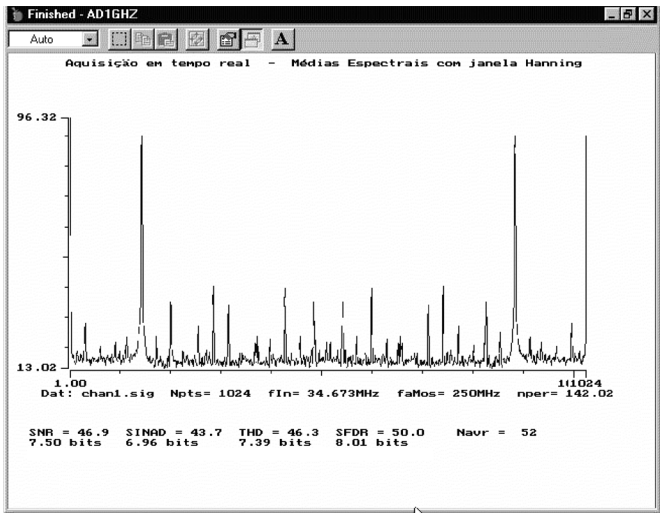

Fig. 8. Averaged DFT of a sinusoidal signal of approximately 34 MHz acquired at 250 MHz by one acquisition channel.

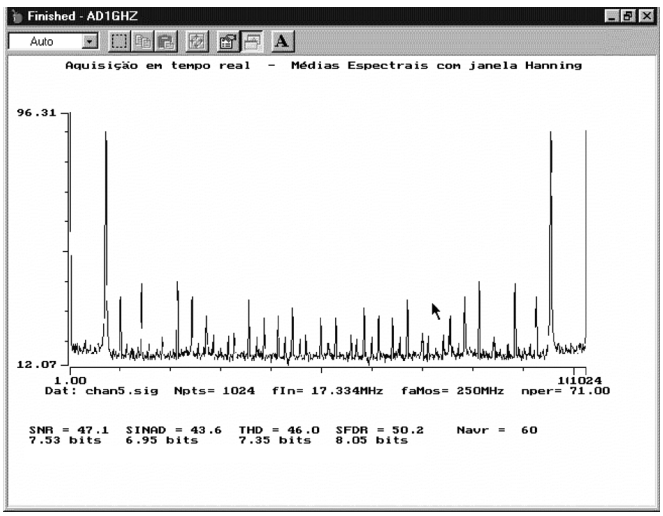

Fig. 9. Averaged DFT of the same sinusoidal signal of Fig. 8 acquired by two interleaved channels conveniently calibrated. Please note the software has been fooled, and thinks the sampling frequency is 250 MHz instead of 500 MHz (and so the input frequency is shown having half its real frequency).

As a result, for the signal used for calibration, the interleaved channels operate very well, as can be seen in Fig. 8 and Fig. 9.

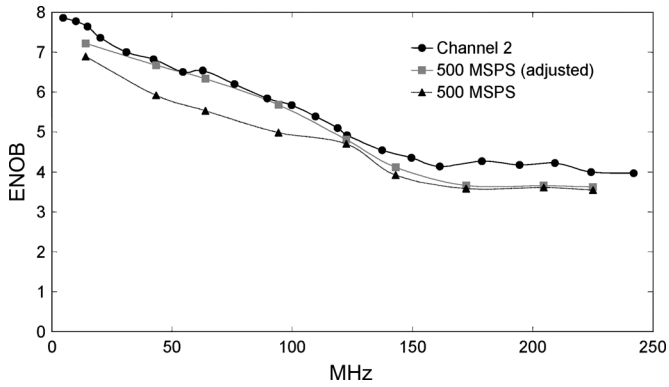

Fig. 10. ENOB of interleaved channel with and without amplitude correction compared to AC2.

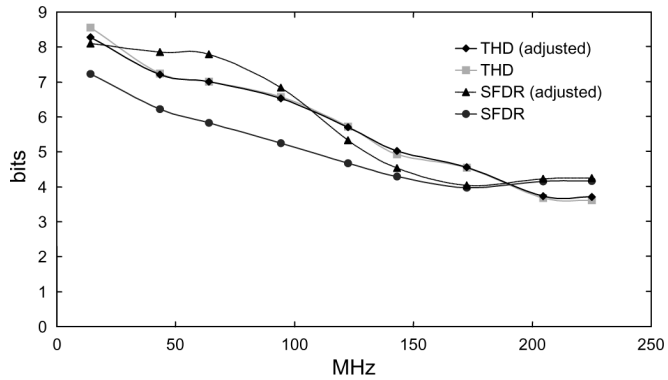

Fig. 11. Effect of the amplitude correction in the THD and SFDR of the interleaved channel.

After calibrating the two interleaved channels an ENOB test was run. The tests quickly showed a major problem of interleaved channels: there are amplitude and phase dependent mismatches that ruin the performance of the overall channel. For the range of frequencies tested mismatches of up to ± 2 lsb and ± 50 ps were found.

Using the information given by DFT interpolating and choosing one channel as standard, a linear adjustment of the offset and amplitude of the other channel is made that helps minimize the problem (Fig. 10). When working with multifrequency signals, this adjustment is based in the spectral line with higher amplitude.

The usefulness of the adjustment in amplitude is apparent in Fig. 11, showing that the amplitude mismatches between channels introduced spurious frequency components in the interleaved channel that were removed by the amplitude adjustment procedure. At higher frequencies the uncorrected phase mismatches dominate and the interleaved channel does not behave as well.

C. Multifrequency Signals

A rectangular signal of an approximate frequency of 5.8 MHz was acquired at 250 MHz with one channel (Fig. 12) and at 500 MHz with two channels interleaved (Fig. 13). The greater detail of the high speed sampling is obvious, although a careful

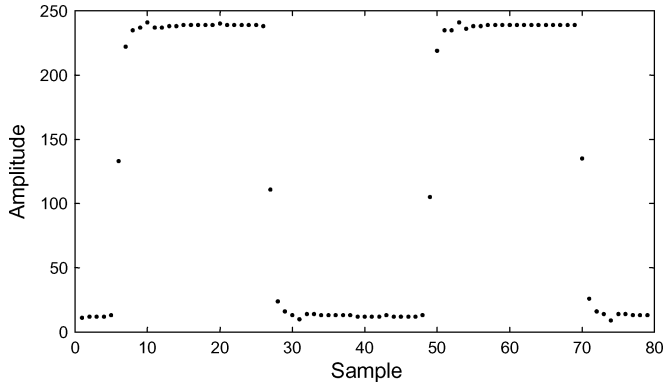

Fig. 12. Rectangular wave sampled at 250 MSPS.

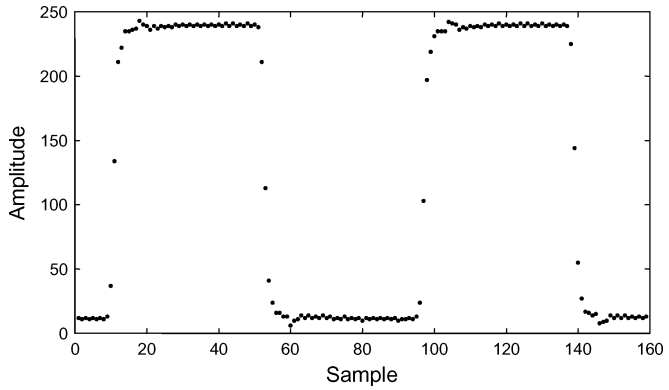

Fig. 13. Rectangular wave sampled at 500 MSPS.

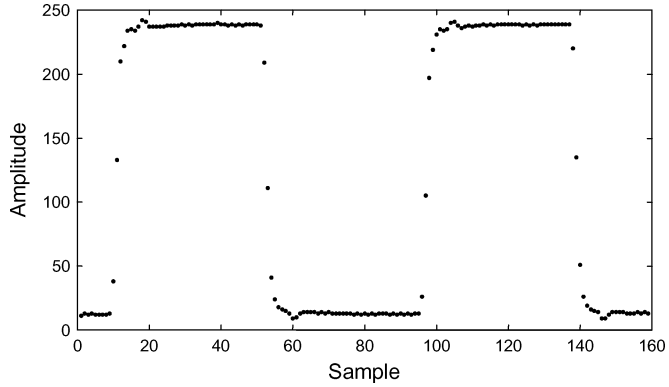

Fig. 14. Rectangular wave sampled at 500 MSPS (amplitude corrected).

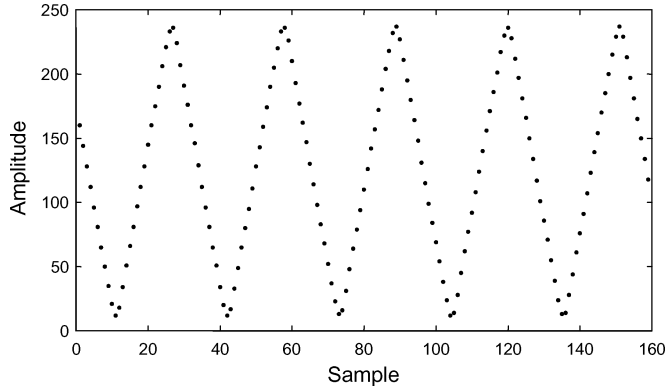

Fig. 15. Triangular wave acquired at 500 MSPS (amplitude corrected).

look allows suspecting from excessive noise that can be quickly related to the interleaved architecture.

By doing amplitude correction based on the amplitude of the fundamental harmonic a more convincing result is obtained (Fig. 14), with most of the high-frequency noise removed (look at the flat zones of the square wave). A triangular wave of approximately 16 MHz acquired at 500 MHz and amplitude-corrected is also given (Fig. 15) showing the very good linear behavior of the interleaved channel (without misplaced points due to amplitude mismatches of the channels).

V. Conclusions

A method has been shown to calibrate in amplitude and time interleaved data acquisition channels. The method uses DFT interpolating to obtain good estimates of the measured signal. The interleaved channels are then time and amplitude matched at a given test frequency. A linear amplitude and offset correction method is suggested capable of improving the acquired signal and correct for amplitude frequency-dependent mismatches.

References

[1] C. F. M. Loureiro, C. M. B. A. Correia, and C. A. F. Varandas, "High-speed multi-input VME bus data acquisition system," *Meas. Sci. Technol.*, vol. 11, pp. 1224–1232, 2000.

[2] A. Silva, L. Cupido, C. Loureiro, S. Vergamota, P. Varela, J. Santos, M. Manso, F. Serra, L. Meneses, M. Tavares, I. Nunes, B. Kurzan, W. Suttrop, and V. Grossman, "New developments of the ASDEX upgrade tokamak microwave reflectometer," *Fusion Eng. Des.*, vol. 46, pp. 389–395, 1999.

[3] F. J. Harris, "On the use of windows for harmonic analysis with the discrete Fourier transform," *Proc. IEEE*, vol. 66, p. 51, 1978.

[4] A. H. Nuttall, "Some windows with very good sidelobe behavior," *IEEE Trans. Acoust., Speech, Signal Process.*, vol. 29, pp. 84–91, 1981.

[5] T. Grandke, "Interpolation algorithms for discrete Fourier-transforms of weighted signals," *IEEE Trans. Instrum. Meas.*, vol. 32, pp. 350–355, 1983.

[6] J. Schoukens, R. Pintelon, and H. Vanhamme, "The interpolated fast Fourier-transform—A comparative-study," *IEEE Trans. Instrum. Meas.*, vol. 41, pp. 226–232, 1992.